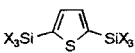
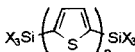
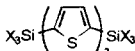
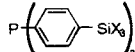
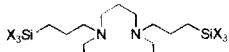
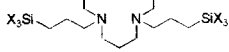
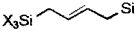
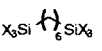




Table 1. Experimental Conditions and Textural Characteristics of Some Xerogels

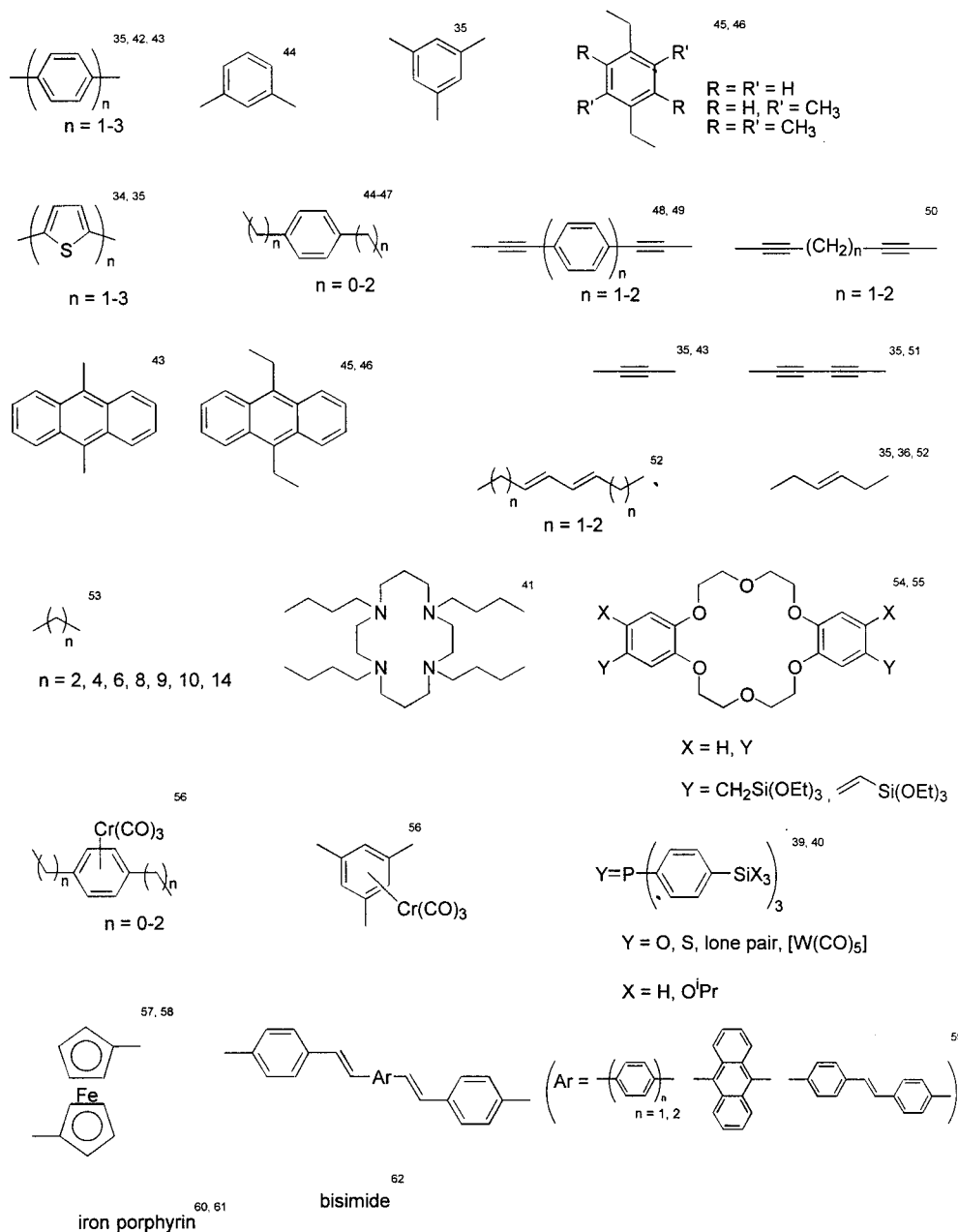
Entry	Precursor	X	Conc. (mole l <sup>-1</sup> )	Solvent	Catalyst (Conc. <sup>a</sup> )	Temp. (°C)	BET S.S.A. (m <sup>2</sup> g <sup>-1</sup> ) <sup>b</sup>
1		OMe	1	MeOH	NH <sub>4</sub> F (1)	20	685
2		OMe	1	THF	NH <sub>4</sub> F (1)	20	20
3		OMe	1	THF	NH <sub>4</sub> F (1)	20	65
4		OMe	1	THF	NH <sub>4</sub> F (1)	20	190
5		O <sup>i</sup> Pr	0.5	THF	TBAF (1)	20	no gel
6		O <sup>i</sup> Pr	0.5	THF	pTSA (1)	20	50
7		O <sup>i</sup> Pr	0.5	THF	HCl (10)	20	460
8		O <sup>i</sup> Pr	0.5	THF	pTSA (1)	110	600
9		H	0.5	THF	TBAF (1)	0	870
10		OEt	1	EtOH	TBAF (1)	20	370
11		OEt	1	EtOH	TBAF (1)	110	800
12		OMe	1	THF	NH <sub>4</sub> F (0.1)	20	20
13		OMe	1	MeOH	NH <sub>4</sub> F (0.1)	20	< 10
14		OMe	3	MeOH	NH <sub>4</sub> F (0.1)	20	325
15		OMe	0.1	MeOH	NH <sub>4</sub> OH (2.6)	20	980
16		OEt	0.4	EtOH	NaOH (10.8)	20	600
17		OEt	0.4	THF	NaOH (10.8)	20	640
18		OEt	0.4	EtOH	HCl (10.8)	20	< 10
19		OEt	0.4	THF	HCl (10.8)	20	380

<sup>a</sup> In molar percentage. <sup>b</sup> Specific surface area.

or metastable (glasses) materials. In sol-gel chemistry, it clearly appears that the experimental conditions used for the hydrolytic polymerization are of drastic influence, and each modification of the parameters results in drastic changes of the characteristics of the final material.<sup>7</sup> It was suggested in the case of silica that even the size of the container may have some influence.<sup>33</sup> At first sight, the characteristics of the solids seem to be controlled by all the parameters able to modify the kinetics of polycondensation. This is illustrated by the examples reported in Table 1 in which the texture is

shown to be a function of the solvent (Table 1, entries 1, 2, 12, 13, and 16–19),<sup>34–38</sup> the organic group (Table 1, entries 2–4),<sup>34</sup> the catalyst (Table 1, entries 5–7 and 16–19),<sup>35–40</sup> the concentration of catalyst<sup>29,34</sup> and of the precursor (Table 1, entries 14 and 15),<sup>36</sup> the leaving group (Table 1, entries 8 and 9),<sup>39,40</sup> and the temperature (Table 1, entries 5, 8, 10, and 11).<sup>40,41</sup> In the case of the hybrid solids, the effect of the kinetic parameters appears to be drastic since the organic part plays a role in the polycondensation reaction which occurs in at least six directions in the case of bis-silylated precursors. A

## Scheme 3. Examples of Organic Units Included in Nanostructured Materials



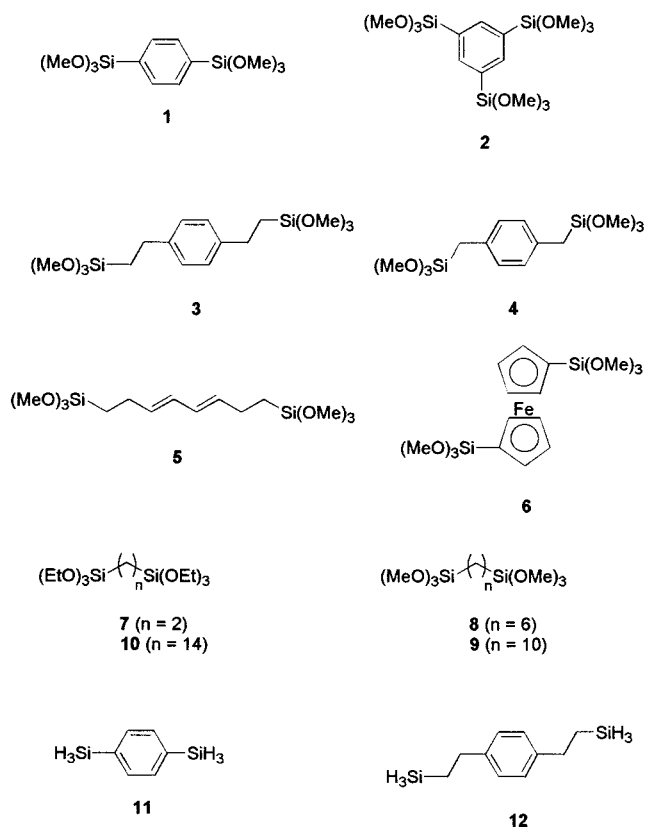
small change in the experimental conditions can lead to a completely different solid. *Furthermore, the reproducibility is difficult to obtain and it is observed only when the experimental conditions and the purity of chemicals are carefully controlled with the precision used in physical chemistry or analytical measurements.*

This paper will focus on the hybrid materials obtained from organic precursors containing at least two Si-C bonds (Scheme 2); the inorganic matrix is built up around the organic moiety through the hydrolytic polycondensation. Most of the organic spacers studied until now are reported in Scheme 3. The use of Si-C bonds provides a stable linkage between the organic unit and the oxide matrix. The most commonly hydrolyzable groups used are trialkoxysilyl groups -Si(OR)<sub>3</sub> with R = Me, Et, <sup>i</sup>Pr. However, -SiCl<sub>3</sub><sup>45,46</sup> and -SiH<sub>3</sub><sup>63,64</sup> groups have also been studied. We have performed a systematic study of the different parameters involved during the hydrolytic polycondensation process, using

organic precursors having different structural features, rigid, semirigid, and flexible (Scheme 4). We present the conclusions we are considering of importance for the control of the texture which is one of the most puzzling aspects of the sol-gel process. We have chosen to work with precursors containing at least two Si(OR)<sub>3</sub> groups instead of monosubstituted R-Si(OR)<sub>3</sub>. The main reason is the difficulty to obtain solids with them without dilution with Si(OR)<sub>4</sub><sup>65</sup> as pointed out recently by Loy.<sup>66</sup>

We present here an overall review of these results which show that the texture of these materials is under kinetic control and illustrate the importance of each parameter. Thus, the influence of the kinetic parameters (nature and concentration of the organic precursor and catalyst, solvent, temperature, and nature of the hydrolyzable group) on the textural properties of the resulting xerogels will be presented. However, we report also the influence of time and temperature of aging which points out the complexity of the problem.

## Scheme 4. Molecular Precursors



## Experimental Results

In this review, we present a selection among the results reported, choosing the most significant examples. The molecular precursors which have been investigated are listed in Scheme 4. They contain organic units with various geometries and structural features: “rigid”, “semi-rigid”, and “flexible” spacers have been studied. A precursor presenting nine directions for polycondensation is also reported and a ferrocene derivative as well. We did not include the results reported by Lindner’s group<sup>22,67,68</sup> since the materials they describe exhibit behavior more similar to cross-linked polymers rather than to silicas. All of them exhibit swelling properties in the presence of organic solvents due to the great lipophilicity of the organic spacer and the use of  $-\text{SiMe}(\text{OR})_2$  instead of  $-\text{Si}(\text{OR})_3$ . In contrast, all the materials reported here present silica-like behavior corresponding to solids which do not exhibit any swelling properties due to the high level of polycondensation of the network in opposition to the greater flexibility of Lindner’s materials.<sup>67,68</sup>

Concerning the “microscopic level”, the spectroscopic methods and particularly solid-state NMR are excellent tools for the study of the organic unit included in the material. Solid state  $^{13}\text{C}$  NMR spectroscopy is a means of identifying the molecular units bound to the matrix (assignment of all the carbon atoms of an organic moiety), while  $^{29}\text{Si}$  NMR spectroscopy provides information about (i) the absence of any Si–C bond cleavage (no Q units corresponding to silica are observed)<sup>69–71</sup> and (ii) the degree of polycondensation around the silicon. CP MAS spectroscopy is not quantitative. However, it has been shown that single-pulse experiments did not reveal any significant variation in relative

intensity from the CP MAS spectra in the case of xerogels prepared from precursors containing different organic groups.<sup>43,53,72</sup> This was attributed to the presence of hydrogen atoms in the close environment of silicon due to the proton-rich organic group attached to it. Thus, it is possible to report here, as a first approximation ( $\pm 5\%$ ), the percentage of the different substructures estimated by deconvolution of spectra which reflect the order of magnitude of polycondensation at silicon. All the molecular precursors investigated until now lead to hybrid solids. In all cases the  $^{13}\text{C}$  and  $^{29}\text{Si}$  CP MAS NMR spectra reveal that the organic group survives the sol–gel polymerizations intact and that no silicon–carbon bond cleavage occurs.

The “macroscopic data” permit determination of the textural characteristics of the materials which correspond to the classical identification of the solids in terms of granulometry, specific surface area, pore volume, porosity, and density. The specific surface areas of xerogels were determined using 35 points adsorption–desorption isotherm plot measurements<sup>73</sup> and were evaluated using the BET equation.<sup>74</sup> The porous volume was determined by the BJH method<sup>75,76</sup> and the microporous volume was evaluated by the analysis of the t-plot diagram. The control of the texture of the xerogels constitutes an important challenge in materials chemistry since it is determining for the properties and applications of the resulting solids.

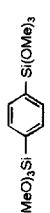
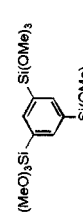
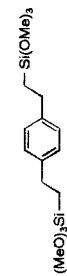
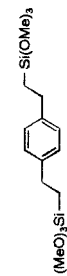
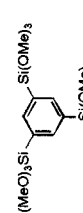
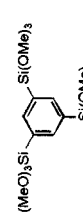
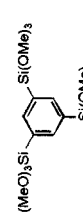
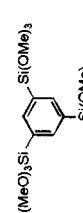
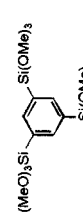
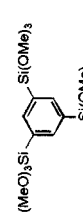
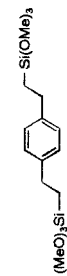
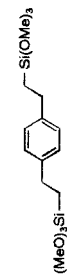
## Influence of the Solvent and the Concentration.

The  $^{29}\text{Si}$  NMR data and the textural characteristics of some xerogels obtained in MeOH and THF at two different concentrations of precursor (0.5 and 1.0 M) with 1% molar of tetrabutylammonium fluoride (TBAF) as catalyst are presented in Table 2.<sup>72,77–79</sup> It emerges from this study that the solvent has a drastic influence in the case of the flexible precursor **3**: highly polycondensed porous solids are obtained in THF, whereas moderate levels of condensation at silicon and nonporous xerogels are formed in MeOH (Table 2, entries 9–12) whatever the concentration. In contrast, the solvent employed for the hydrolysis polycondensation reaction has a weak influence on both the structural and textural properties of the solid obtained from the “rigid” precursors **1** and **2**. In this case, an increase of the concentration of precursor induces an increase of specific surface area only in MeOH (Table 2, entries 3, 4, 7, and 8).

The results presented in Table 2 show that the solvent and the concentration of the precursor have an influence on the characteristics of the xerogels prepared under nucleophilic catalysis (TBAF). It was of interest to investigate other types of catalysts.

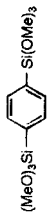
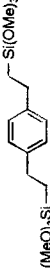
**Influence of the Catalyst.** Usually, the sol–gel polymerization of organic molecular precursors is catalyzed by nucleophiles (fluoride ions), acids, or bases. To highlight the kinetic control of the hydrolytic process, we have compared the effect of the usual ionic catalysts with the nonionic ones. Study has been performed more particularly by comparing the “rigid” **1** and “flexible” **3** precursors in MeOH and THF. Ionic catalysts (TBAF,  $\text{NH}_4\text{F}$ ,  $\text{NH}_4\text{OH}$ ,  $\text{NaOH}$ , and  $\text{HCl}$ ) and nonionic ones such as DMF (dimethylformamide), DMAP ((dimethylamino)pyridine), NMI (*N*-methylimidazole), and HMPT (hexamethylphosphorotriamide) have been investigated.<sup>78–80</sup>

Table 2. Structural and Textural Characteristics of Xerogels Obtained from 1, 2, and 3 with 1% Molar of TBAF at +20 °C

Entry	Precursor	Solvent	Conc. (M)	<sup>29</sup> Si NMR (%)				Cond. <sup>a</sup>	S.S.A. (m <sup>2</sup> g <sup>-1</sup> ) <sup>b</sup>	BET	
				T <sup>0</sup>	T <sup>1</sup>	T <sup>2</sup>	T <sup>3</sup>			μ-pores (%) <sup>c</sup>	Size (Å) <sup>d</sup>
1		THF	0.5	0	16	64	20	67	1300	10	20-120 <sup>e</sup>
2		THF	1.0	0	16	62	22	68	1240	20	20-120 <sup>e</sup>
3		MeOH	0.5	0	19	63	18	66	550	60	35
4		MeOH	1.0	0	20	65	15	65	1050	40	20-120 <sup>e</sup>
5		THF	0.5	0	27	56	17	64	760	10	20-120 <sup>e</sup>
6		THF	1.0	0	20	65	15	65	880	10	20-120 <sup>e</sup>
7		MeOH	0.5	0	32	55	13	61	770	10	20-120 <sup>e</sup>
8		MeOH	1.0	0	30	60	10	60	1155	10	60
9		THF	0.5	0	0	38	62	87	565	25	20-120 <sup>e</sup>
10		THF	1.0	0	0	43	57	84	530	50	20-70 <sup>e</sup>
11		MeOH	0.5	6	27	44	23	61	<10	-	-
12		MeOH	1.0	2	30	55	13	60	<10	-	-

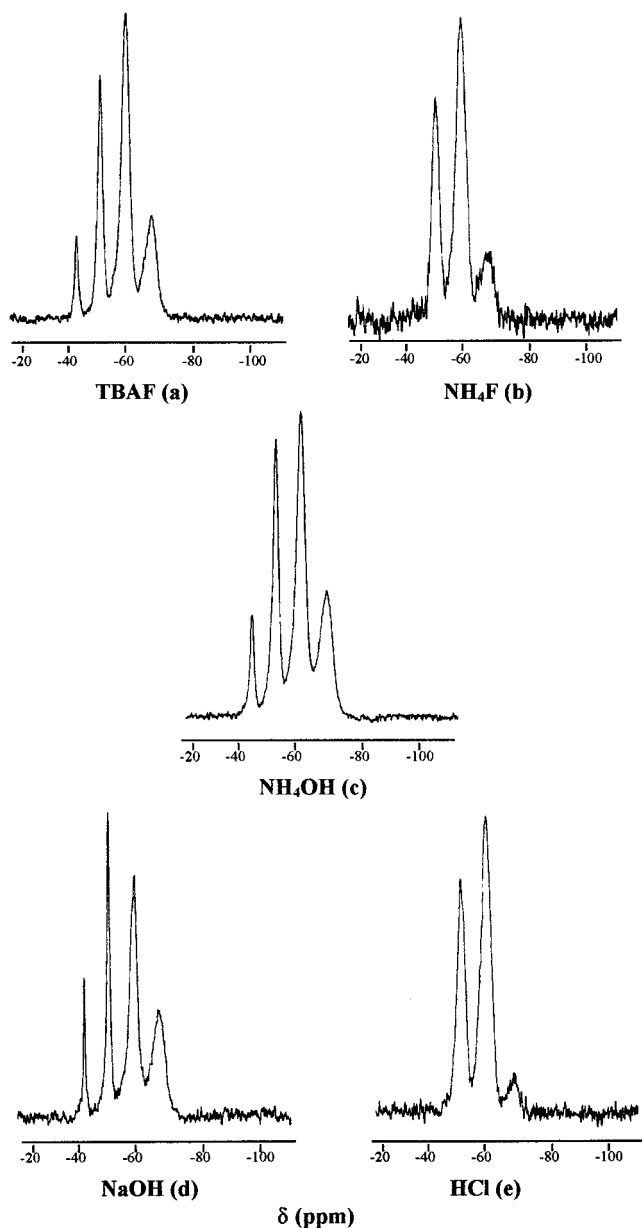
<sup>a</sup> Level of condensation. <sup>b</sup> Specific surface area. <sup>c</sup> Percentage of micropores. <sup>d</sup> Size of mesopores. <sup>e</sup> No narrow pore size distribution.

Table 3. Structural and Textural Characteristics of Xerogels Obtained from 1 and 3 in THF (0.5 M) with 1% Molar of Ionic or Nonionic Catalysts at +20 °C

Entry	Precursor	Catalyst	<sup>29</sup> Si NMR (%)				Cond. <sup>b</sup>	S.S.A. (m <sup>2</sup> g <sup>-1</sup> ) <sup>c</sup>	μ-pores (%) <sup>d</sup>	Size (Å) <sup>e</sup>
			T <sup>0</sup>	T <sup>1</sup>	T <sup>2</sup>	T <sup>3</sup>				
1		TBAF	0	16	64	20	67	1300	10	20-120 <sup>e</sup>
2	1	NH <sub>4</sub> F	0	20	65	15	65	390	80	20-120 <sup>e</sup>
3	1	NH <sub>4</sub> OH	0	20	63	17	67	385	80	20-120 <sup>e</sup>
4	1	NaOH	0	24	64	12	63	530	75	20-120 <sup>e</sup>
5	1	HCl	0	21	65	14	64	540	80	20-120 <sup>e</sup>
6	1	DMAP	5	30	34	31	64	670	65	20-70 <sup>e</sup>
7	1	HMPT	8	25	43	24	61	<10	-	-
8		TBAF	0	0	38	62	87	565	25	20-120 <sup>e</sup>
9	3	NH <sub>4</sub> F	1	14	49	36	73	<10	-	-
10	3	NH <sub>4</sub> OH	f	f	f	f	f	f	f	f
11	3	NaOH	0	9	34	57	83	<10	-	-
12	3	HCl	0	21	65	14	64	<10	-	-
13	3	DMAP	10	17	35	38	67	<10	-	-
14	3	HMPT	0	30	60	10	60	<10	-	-

<sup>a</sup> Level of condensation. <sup>b</sup> Specific surface area. <sup>c</sup> Percentage of micropores. <sup>d</sup> Size of mesopores. <sup>e</sup> No narrow pore size distribution. <sup>f</sup> No gel.





**Figure 1.**  $^{29}\text{Si}$  CP MAS NMR spectra of xerogels obtained from **3** in MeOH (0.5 M) with 1% molar of catalyst.

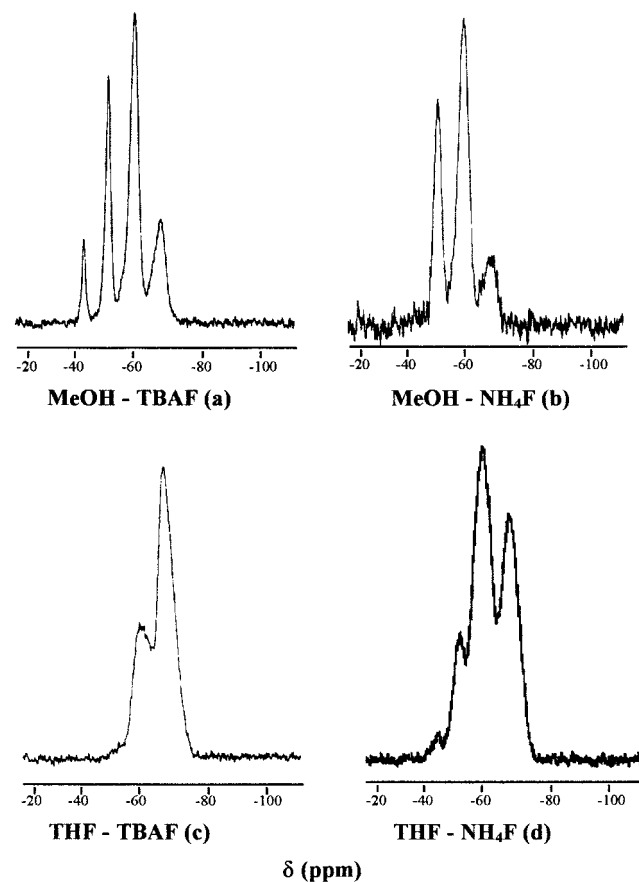
The most representative results are summarized in Table 3.

The structural and textural properties of the xerogels obtained from **1** are poorly influenced by both the solvent and the catalyst: porous solids with high specific surface area and a large microporous contribution are always obtained.<sup>78,80</sup> The level of condensation at silicon lay in the range 60–67% in all cases (Table 3, entries 1–7). In contrast, the catalyst and the solvent have a great influence on the properties of the xerogels obtained from the “flexible” precursor **3**. Ionic catalysts lead to more polycondensed xerogels (73–87%) than nonionic ones (59–68%) in THF (with the exception of  $\text{NH}_4\text{OH}$ ; Table 3, entry 10), whereas in MeOH the level of condensation is in the range 59–63%.<sup>78,80</sup> Figure 1 shows the  $^{29}\text{Si}$  CP MAS NMR spectra of xerogels obtained from **3** in MeOH with ionic catalysts. Interestingly, a porous solid with a high specific surface area is formed only with TBAF in THF (Table 3, entry 8), when in the same conditions, a totally different solid is

obtained using  $\text{NH}_4\text{F}$  (Table 3, entry 9). An illustration of this difference is exemplified by a comparison of the  $^{29}\text{Si}$  CP MAS NMR spectra of these xerogels given in Figure 2.

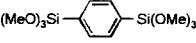
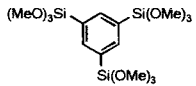
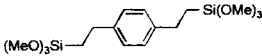
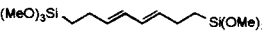
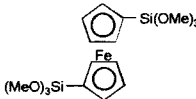
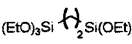
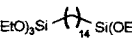
Besides the strong influence of the catalyst, these results suggest that the organic group is of great importance.

**Influence of the Organic Group.** Organic spacers having different structural features have been investigated (Scheme 4).<sup>72,79</sup> Compounds **7** and **10** bear a triethoxysilyl group. It has been shown that changing the  $\text{Si}(\text{OMe})_3$  group by the  $\text{Si}(\text{OEt})_3$  group resulted only in longer gel times for ethoxy groups. The same conditions (0.5 M in THF with 1% molar of TBAF at +20 °C) have been chosen since flexible compound **3** exhibits porosity only in these conditions. The main results arising from this study are given in Table 4. Highly polycondensed (86–95%) solids are formed in the case of “flexible” precursors (Table 4, entries 3, 4, and 7). These very high levels of condensation could certainly be due to the flexibility of the organic moiety (especially for **10**) which might facilitate the polycondensation reaction and the cross-linking of the network. Another explanation could be that there is a lack of organization in the case of long alkylene chains, requiring a higher level of condensation to form a solid. In most cases, the solids presented high specific surface areas with a weak microporous contribution (5–25%) and mesopores with no narrow pore size distribution. In the case of alkylene bridging groups, increasing the length of the chain drastically modifies the texture of the xerogels; a decrease of the specific surface area and the micropores



**Figure 2.**  $^{29}\text{Si}$  CP MAS NMR spectra of xerogels obtained from **3** (0.5 M) with 1% molar of catalyst.

**Table 4. Structural and Textural Characteristics of Xerogels Obtained from Different Precursors in THF (0.5 M) with 1% Molar of TBAF at +20 °C**

Entry	Precursor	<sup>29</sup> Si NMR (%)					BET			
		T <sup>0</sup>	T <sup>1</sup>	T <sup>2</sup>	T <sup>3</sup>	Cond. <sup>a</sup>	S.S.A. (m <sup>2</sup> g <sup>-1</sup> ) <sup>b</sup>	μ-pores (%) <sup>c</sup>	Size (Å) <sup>d</sup>	
1		0	16	64	20	67	1300	10	20-120 <sup>e</sup>	
	<b>1</b>									
2		0	27	56	17	64	760	10	20-120 <sup>e</sup>	
	<b>2</b>									
3		0	0	38	62	87	565	25	20-120 <sup>e</sup>	
	<b>3</b>									
4		0	9	23	68	86	665	10	20-60 <sup>e</sup>	
	<b>5</b>									
5		f	f	f	f	f	25	30	20-120 <sup>e</sup>	
	<b>6</b>									
6		f	f	f	f	f	795	60	20-120 <sup>e</sup>	
	<b>7</b>									
7		0	0	16	84	95	< 10	-	-	
	<b>10</b>									

<sup>a</sup> Level of condensation. <sup>b</sup> Specific surface area. <sup>c</sup> Percentage of micropores. <sup>d</sup> Size of mesopores. <sup>e</sup> No narrow pore size distribution. <sup>f</sup> Broad signal.

contribution are observed<sup>79</sup> and the longest precursor leads to a nonporous solid (Table 4, entry 7). A similar result has been observed in other experimental conditions.<sup>53</sup>

It was proposed that this effect might result from the increase in flexibility of these groups that can aggregate and compact more closely.<sup>81</sup> However, the organic group can modify the kinetics of reaction at silicon by steric and electronic effects due to the Si-C bond.

**Influence of the Temperature.** The preparation of xerogels is generally performed at +20 °C. A systematic study of the effect of the temperature has been investigated by varying the temperature from -20 to +55 °C. Experiments were also performed in sealed tubes at +110 °C.<sup>79,82</sup> The different precursors (Scheme 4) were investigated and the hydrolytic process was catalyzed by ionic and nonionic catalysts.<sup>79</sup> The main results, reported in Table 5, clearly show how much the texture of the xerogels is temperature dependent. An increase of the temperature leads to an increase of the mesoporosity and the specific surface area corresponding to a decrease of the microporosity. The adsorption-desorption isotherms for xerogels obtained from **1** (Table 5, entries 1-4) at different temperatures illustrate this result very well (Figure 3). At the low temperatures -20 °C (Figure 3a) and 0 °C (Figure 3b), the isotherms are of type I, indicating a largely microporous solid with a

low mesoporous contribution, though vestiges of hysteresis loops characteristic of capillary filling of mesopores are evident. When the temperature rises to +20 °C (Figure 3c), the isotherm is characteristic of type IV, the microporous volume is only 10%, and the mesopores range between 20 and 120 Å. At +55 °C only 5% of micropores is present and the mesopores show a narrow pore size of 55 Å (Figure 3d). When the gels are formed at +110 °C, they are generally mesoporous with a narrow pore size.<sup>79</sup> It also appears that the texture of the material is not directly correlated to the degree of polycondensation at silicon since only minor variations are observed when the temperature is increased (Table 5). A similar observation has been reported in the case of phosphine or azamacrocyclic precursors.<sup>40, 41</sup>

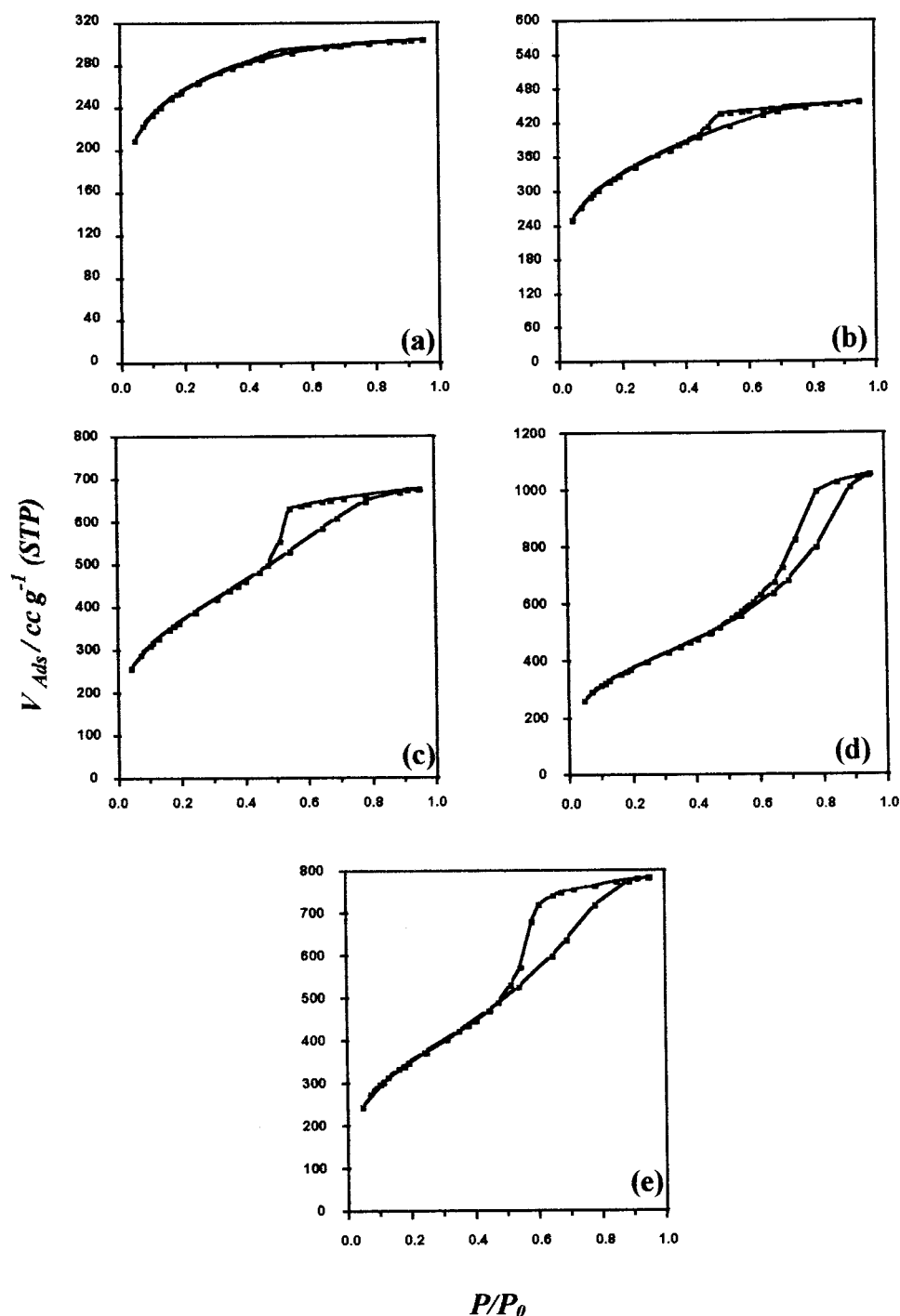
**Influence of the Aging Conditions.** Generally, the gels are aged for 6 days. Since a drastic effect of temperature is observed on the texture of the xerogels, it was of great interest to change the conditions of aging, varying the length and the temperature.<sup>83</sup> Selected results are given in Table 6. It clearly appears that polycondensation at silicon is only poorly influenced by the length of aging; a weak increase of the level of condensation is observed. In contrast, the length and the temperature of aging have a drastic effect for both the specific surface area and the porosity. For a given temperature, increasing the time of aging induces an



Table 5. Structural and Textural Characteristics of Xerogels Obtained from 1, 2, 3, 5, and 10 (0.5 M) at Several Temperatures with 1% Molar of Ionic and Nonionic Catalysts

Entry	Precursor	Solvent	Catalyst	Temp. (°C)	<sup>29</sup> Si NMR (%)				Cond. <sup>a</sup>	S.S.A. (m <sup>2</sup> g <sup>-1</sup> ) <sup>b</sup>	μ-pores (%) <sup>c</sup>	Size (Å) <sup>d</sup>
					T <sup>0</sup>	T <sup>1</sup>	T <sup>2</sup>	T <sup>3</sup>				
1		THF	TBAF	-20	0	18	49	33	71	900	55	20-120 <sup>e</sup>
2	1			+20	0	16	64	20	67	1300	10	20-120 <sup>e</sup>
3				+55	0	18	42	40	74	1300	5	55
4				+110	0	13	47	40	76	1230	5	45
5			DMAP	-20	7	39	28	26	58	<10	-	-
6				+30	5	30	34	31	64	680	65	20-70 <sup>e</sup>
7				+55	5	32	35	28	62	580	55	20-120 <sup>e</sup>
7		MeOH	TBAF	-20	0	28	53	19	64	470	20	20-70 <sup>e</sup>
8	7			+20	0	32	55	13	61	770	10	20-120 <sup>e</sup>
9				+55	0	17	56	27	70	1220	5	50-90
10	2			+110	0	22	53	25	68	950	0	105
11				-20	0	0	55	45	82	<10	-	-
12				+20	0	0	38	62	87	565	25	20-120 <sup>e</sup>
13				+55	0	0	59	41	80	700	5	40
14				+110	0	0	57	43	81	780	0	100
15			HCl	+20	0	8	64	28	73	<10	-	-
16				+55	0	15	52	33	73	<10	-	-
17												
18		THF	TBAF	-20	0	8	42	50	81	250	20	20-50 <sup>e</sup>
19	18			+20	0	9	23	68	86	665	10	20-60 <sup>e</sup>
20				+55	0	0	25	75	91	870	5	35, 60
21				+110	0	0	21	79	93	920	0	35, 55, 80
22		THF	TBAF	-20	4	0	34	62	85	<10	-	-
23	22			+20	0	0	16	84	95	<10	-	-
24				+55	0	0	9	91	97	<10	-	-

<sup>a</sup> Level of condensation. <sup>b</sup> Specific surface area. <sup>c</sup> Percentage of micropores. <sup>d</sup> Size of mesopores. <sup>e</sup> No narrow pore size distribution.

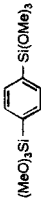
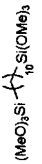


**Figure 3.**  $N_2$  adsorption–desorption isotherms of xerogels obtained from **1** in THF (0.5 M) with 1% molar of TBAF at (a)  $-20\text{ }^\circ\text{C}$ , (b)  $0\text{ }^\circ\text{C}$ , (c)  $+20\text{ }^\circ\text{C}$ , (d)  $+55\text{ }^\circ\text{C}$ , and (e)  $+110\text{ }^\circ\text{C}$ .

increase of the specific surface area and an increase of mesoporosity (Table 6). This phenomenon could be explained by the elimination of the surface roughness with the remainder of the mesopores. The same behavior is observed whatever the solvent or the structure of the organic group.<sup>83</sup> A noteworthy illustration of the influence of aging conditions is shown in Figure 4. The  $N_2$  adsorption–desorption isotherms of the four xerogels obtained from **1** point out the drastic influence, on the texture, of aging conditions and especially the temperature. This behavior is observed with all the catalysts.

However, a particular behavior is evidenced only with NaOH.<sup>84</sup> The  $^{29}\text{Si}$  CP MAS NMR data reported in Table 7 clearly show that the percentages of the different  $T^i$  substructures highly depend on the aging conditions, whereas the overall order of magnitude of polycondensation at silicon is very similar whatever the conditions. A comparison between the xerogels (Table 7) shows that, for a given temperature, varying the length of aging (entries 3 and 5) or increasing the temperature of aging (entries 3 and 6) induces considerable changes in  $T^i$  repartition, and especially  $T^0$  site population reforms

Table 6. Structural and Textural Characteristics of Xerogels Obtained from 1 and 9 in THF (0.5 M) with 1% Molar of Catalyst at +20 °C for the Temperature of Gelation and for the Temperature of Aging

Entry	Precursor	Catalyst	Ageing (days)	<sup>29</sup> Si NMR (%)				Cond. <sup>a</sup>	S.S.A. (m <sup>2</sup> g <sup>-1</sup> ) <sup>b</sup>	BET	
				T <sup>0</sup>	T <sup>1</sup>	T <sup>2</sup>	T <sup>3</sup>			μ-pores (%) <sup>c</sup>	Size (Å) <sup>d</sup>
1		TBAF	0	0	18	55	27	70	940	30	20-60 <sup>e</sup>
2	1		6	0	16	64	20	67	1300	10	20-120 <sup>e</sup>
3	1		15	0	7	66	27	73	1370	6	20-80 <sup>e</sup>
4	1		30	0	13	54	33	73	1430	5	45
5	1		90	0	9	52	39	77	1385	5	20-50 <sup>e</sup>
6		HCl	0	0	38	62	0	54	<10	-	-
7			3	0	40	51	14	56	<10	-	-
8			6	0	21	65	14	64	540	80	20-120 <sup>e</sup>
9			15	0	31	51	18	62	185	65	20-120 <sup>e</sup>
10			30	0	32	60	8	59	35	30	20-120 <sup>e</sup>
11		DMAP <sup>f</sup>	0	9	28	37	26	60	<10	-	-
12			3	9	28	37	26	60	475	65	20-60 <sup>e</sup>
13			6	5	30	34	31	64	680	65	20-70 <sup>e</sup>
14			15	0	27	45	28	67	875	45	20-50 <sup>e</sup>
15			30	0	21	49	30	70	1160	15	20-50 <sup>e</sup>
16		TBAF	0	5	1	28	66	85	<10	-	-
17	9		6	0	0	27	73	91	290	5	20-70 <sup>e</sup>
18	9		15	0	0	35	65	88	350	5	20-70 <sup>e</sup>
19	9		30	0	0	27	73	91	410	0	45

<sup>a</sup>Level of condensation. <sup>b</sup>Specific surface area. <sup>c</sup>Percentage of micropores. <sup>d</sup>Size of mesopores. <sup>e</sup>No narrow pore size distribution. <sup>f</sup>Temperature of gelation and temperature of aging equal to +30 °C.

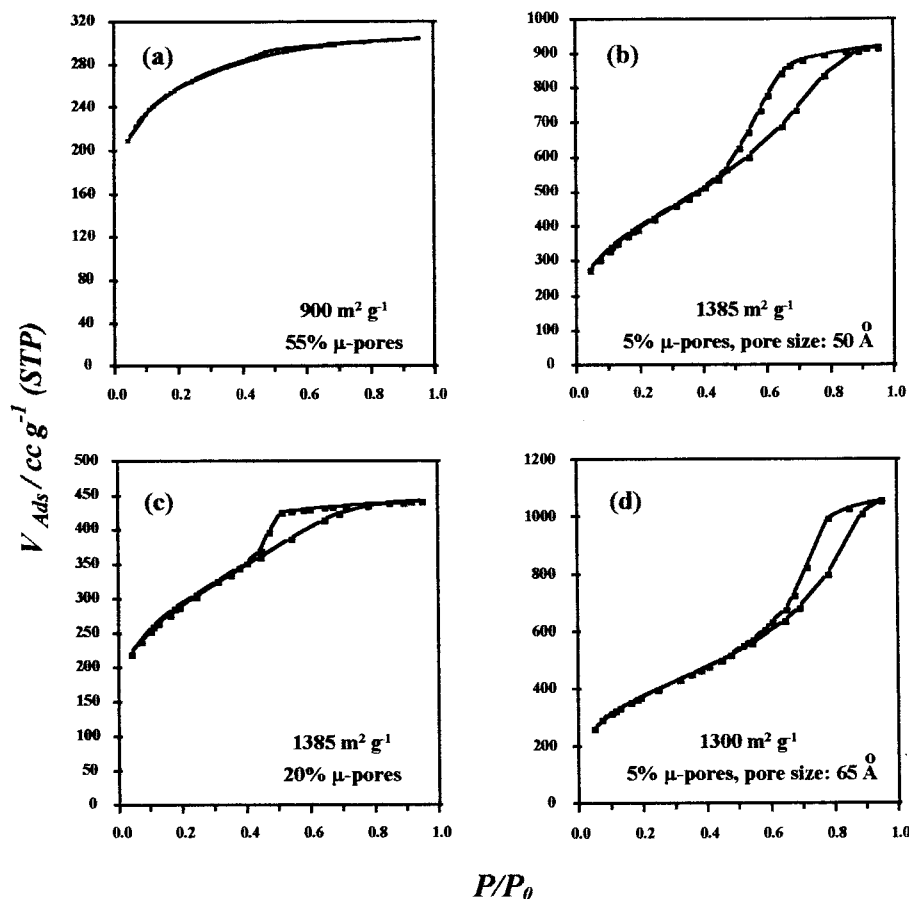


**Figure 4.**  $N_2$  adsorption–desorption isotherms of xerogels obtained from **1** in THF (0.5 M) with 1% molar of TBAF after 6 days of aging: (a) gel at  $-20\text{ }^\circ\text{C}$  and aging at  $-20\text{ }^\circ\text{C}$ , (b) gel at  $-20\text{ }^\circ\text{C}$  and aging at  $+55\text{ }^\circ\text{C}$ , (c) gel at  $+55\text{ }^\circ\text{C}$  and aging at  $-20\text{ }^\circ\text{C}$ , and (d) gel at  $+55\text{ }^\circ\text{C}$  and aging at  $+55\text{ }^\circ\text{C}$ .

during aging. This is the result of redistribution reactions due to the Si–O–Si bond cleavages catalyzed by  $\text{OH}^-$  as shown in Scheme 5.<sup>84</sup>

Taking into account all the results obtained with different organic groups (Table 4) by varying the experimental conditions (Tables 5 and 6), for a given organic structure, it is possible to adjust the synthetic parameters to control the textural properties: meso- or microporosity and high or low specific surface area.

**Influence of the Functionality in Silicon.** The hydrolytic condensation of Si–H of trihydrosilanes is an alternative route to the obtention of silsesquioxane materials.<sup>63,64</sup> The interest in this method is to avoid the formation of alcohol or acids since the leaving group is removed as hydrogen gas.

The precursors **11** and **12** (Scheme 4) having respectively the “rigid” and “flexible” organic group have been hydrolyzed in THF with TBAF as the catalyst.<sup>64</sup> The degree of condensation at silicon cannot be deduced from deconvolution of  $^{29}\text{Si}$  CP MAS NMR spectra because of the presence of hydrogen atoms directly attached to silicon. The xerogels obtained were in both cases mainly mesoporous with high specific surface areas (Table 8, entries 2, 3, 7, and 8). These results show that changing the leaving group in silicon mainly modifies the porosity of the solids (Table 8, entries 1 and 6).

### Discussion

The results discussed here exhibit, without any ambiguity, a parallelism between the experimental

conditions and the texture (specific surface area and porosity) of the solids which are always obtained with complete reproducibility. The experimental conditions and the controlling parameters of the kinetics of polycondensation at silicon are well defined. The variations induced by the nature of the solvent,<sup>72,77–79</sup> of the catalyst,<sup>78–80</sup> of the organic unit,<sup>72,79</sup> and of the leaving group,<sup>64</sup> the effect due to the temperature,<sup>79,82</sup> the influence of concentrations of all reagents,<sup>72,77–79</sup> and finally the great influence of aging<sup>83,84</sup> have been studied. On the basis of all experimental facts, it is possible to conclude that the macroscopic parameters which describe the texture of the solids are under kinetic control. Thus, the hybrid materials are best described as kinetically controlled materials than as unstable solids.<sup>7</sup> The great influence observed with the nature of the organic group is particularly illustrative. The possible explanations are the obvious changes in the kinetics of polycondensation at silicon due to steric and electronic effects. Moreover, the possible interactions between the organic units which have been evidenced by X-ray diffraction<sup>85</sup> and birefringence<sup>86</sup> experiments can also be of great importance in the control of the texture. Their instability is due to the reactivity at the surface or in the bulk when the solids are in contact with reagents (humidity of the air, for instance). However, it is possible to find ways to protect the materials against evolution. We have observed that the xerogels are stable when they are stored in sealed tubes under vacuum.<sup>52</sup> In contrast, most of the nanostructured

Table 7. Structural and Textural Characteristics of Xerogels Obtained from 1 in THF (0.5 M) with 1% Molar of NaOH at Several Times of Aging and Several Temperatures

Entry	Ageing		<sup>29</sup> Si NMR (%)						BET	
	Temp. (°C)	Ageing (days)	T <sup>0</sup>	T <sup>1</sup>	T <sup>2</sup>	T <sup>3</sup>	Cond. <sup>b</sup>	S.S.A. (m <sup>2</sup> g <sup>-1</sup> ) <sup>c</sup>	μ-pores (%) <sup>d</sup>	Size (Å) <sup>e</sup>
1	-20	-20	f	f	f	f	f	f	f	f
2	+20	0	12	21	38	29	61	180	50	20-120 <sup>g</sup>
3		6	0	24	64	12	62	530	75	20-120 <sup>g</sup>
4		15	8	32	33	27	60	520	60	20-120 <sup>g</sup>
5		30	4	32	37	27	62	595	50	20-70 <sup>g</sup>
6	+20	+55	10	26	31	33	62	520	60	20-50 <sup>g</sup>
7	+55	+55	5	18	44	33	65	300	55	20-120 <sup>g</sup>

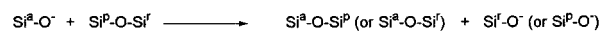
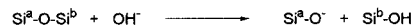
<sup>a</sup> Temperature of gelation. <sup>b</sup> Level of condensation. <sup>c</sup> Specific surface area. <sup>d</sup> Percentage of micropores. <sup>e</sup> Size of mesopores. <sup>f</sup> No gel after several months. <sup>g</sup> No narrow pore size distribution.

### Scheme 5. NaOH Catalysis

#### a) Polycondensation



#### b) Si-O-Si bond cleavage and redistribution reactions



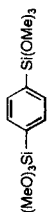
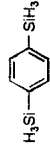
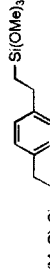
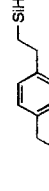
hybrid materials exhibit evolution of the textural properties upon standing in air. The texture appears very sensitive to moisture.

If we consider now the classical scheme which represents the different steps in the sol-gel process (Scheme 6), it is not possible to propose any step as the controlling step of the texture of the solid. Two pieces of experimental evidence are showing the complexity of the problem: (1) The effect of the temperature is drastic for the value of both specific surface area and porosity. However, the polycondensation at silicon measured by <sup>29</sup>Si NMR is poorly dependent on the temperature.<sup>79,82</sup> This observation suggests that polycondensation at silicon is not an important factor for the control of the textural parameters (specific surface area and porosity). Thus, we conclude that polycondensation at silicon and texture are certainly not controlled in the same step of the overall process, which leads to the polysilsesquioxane from the precursor through the colloidal sol formation (Scheme 6). (2) The drastic effect of the temperature observed during aging is also very informative. Indeed, aging corresponds to a transformation occurring on the solid material. It takes place after the sol-gel transition. Thus, it is not directly connected to the first chemical steps of polycondensation occurring in solution and it operates on solid materials which are already highly cross-linked. That means that the control of the texture of the material is also highly dependent on the evolution of the solid itself. (3) The nature of the organic unit seems to be of great importance for polycondensation at silicon. However, for a given organic structure, it is possible to control the texture by changing the experimental conditions: the temperature, nature of the solvent, catalyst, etc. can be considered as parameters with which it is possible to play for reaching a suitable texture.

### Conclusion and Perspectives

Thus, in this step of the work, it is possible to conclude that the textural features of the materials (specific surface area and porosity) are under the control of the parameters which are of importance in the kinetics of polycondensation. In our opinion, these conclusions may be extended to solids obtained by sol-gel techniques from R-Si(OR)<sub>3</sub> and also from Si(OR)<sub>4</sub>. However, a better understanding of both the formation and evolution of materials involves complementary studies. Indeed, the results obtained in aging the gels at different temperatures suggest that the different steps of the sol-gel solid formation are not controlled by the same parameters. For instance, the degree of polycondensa-

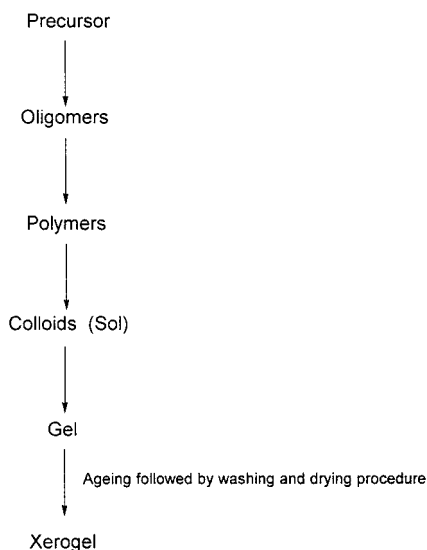
Table 8. Textural Characteristics of Xerogels Obtained from 11 and 12 in THF at 0 °C

Entry	Precursor	Concentration (mole l <sup>-1</sup> )	Catalyst (Conc. <sup>a</sup> )	BET		
				S.S.A. (m <sup>2</sup> g <sup>-1</sup> ) <sup>b</sup>	μ-pores (%) <sup>c</sup>	Size (Å) <sup>d</sup>
1		0.5	TBAF (1.0)	1150	40	20-120 <sup>e</sup>
2		0.5	TBAF (0.1)	930	5	20-80 <sup>e</sup>
3		1.0	TBAF (0.1)	1200	0	50
4		0.5	CIRh(PPh <sub>3</sub> ) <sub>3</sub> (0.1)	55	30	20-120 <sup>e</sup>
5		1.0	CIRh(PPh <sub>3</sub> ) <sub>3</sub> (0.1)	360	25	20-60 <sup>e</sup>
6		0.5	TBAF (1.0)	165	30	20-120 <sup>e</sup>
7		0.5	TBAF (0.1)	360	5	20-80 <sup>e</sup>
8		1.0	TBAF (0.1)	495	5	20-50 <sup>e</sup>
9		0.5	CIRh(PPh <sub>3</sub> ) <sub>3</sub> (0.1)	100	0	20-90 <sup>e</sup>
10		1.0	CIRh(PPh <sub>3</sub> ) <sub>3</sub> (0.1)	520	10	20-50 <sup>e</sup>

<sup>a</sup> Molar percentage. <sup>b</sup> Specific surface areas. <sup>c</sup> Percentage of micropores. <sup>d</sup> Size of mesopores. <sup>e</sup> No narrow pore size distribution.



## Scheme 6. General Scheme of the Sol–Gel Process



tion at silicon is not temperature dependent when the porosity is highly dependent on the aging temperature. These observations suggest that more information must be collected, looking to other properties such as the short-range or long-range order by studying other parameters (SAXS, NMR, birefringence, etc.) to try to discriminate the factors which are controlling the different steps of the solid formation as shown in Scheme 6.

## References

- (1) Rouxel, J. *Chem. Scr.* **1988**, *28*, 33.
- (2) Livage, J. *Chem. Scr.* **1988**, *28*, 9.
- (3) Bradley, D. C.; Mehrotra, R. C.; Gaur, D. P. *Metal Alkoxides*; Academic Press: New York, 1978.
- (4) Livage, J.; Henry, M.; Sanchez, C. *Prog. Solid State Chem.* **1988**, *18*, 259.
- (5) Yajima, S.; Hayashi, J.; Omori, M. *Chem. Lett.* **1975**, 931.
- (6) Yajima, S.; Okamura, K.; Hayashi, J. *Chem. Lett.* **1975**, 1209.
- (7) Brinker, C. J.; Scherer, G. W. *Sol–Gel Science: The Physics and Chemistry of Sol–Gel Processing*; Academic Press: San Diego, 1990.
- (8) Corriu, R. J. P.; Leclercq, D.; Vioux, A.; Pauthe, M.; Phalippou, J. *Ultrastructure Processing of Advanced Ceramics*; Mackenzie, J. D., Ulrich, D. R., Eds.; Wiley: Chichester, 1988; p 113.
- (9) Iler, R. K. *The Chemistry of Silica*; Wiley: New York, 1979.
- (10) Hench, L. L.; West, J. K. *Chem. Rev.* **1990**, *90*, 33.
- (11) Chojnowski, J.; Cypryk, M.; Kazmierski, K.; Rozga, K. *J. Non-Cryst. Solids* **1990**, *125*, 40.
- (12) Sefcik, J.; Cormick, A. V. *Catal. Today* **1997**, *35*, 205.
- (13) Pouxviel, J. C.; Boilot, J. P.; Beloeil, J. C.; Lallemand, J. Y. *J. Non-Cryst. Solids* **1987**, *89*, 345.
- (14) Devreux, F.; Boilot, J. P.; Chaput, F.; Lecomte, A. *Phys. Rev. A* **1990**, *41*, 6901.
- (15) Malier, L.; Boilot, J. P.; Chaput, F.; Devreux, F. *Phys. Rev. A* **1992**, *46*, 959.
- (16) Rankin, S. E.; Sefcik, J.; McCormick, A. V. *J. Phys. Chem. A* **1999**, *103*, 4233.
- (17) Schmidt, H. K. *Mater. Res. Soc. Symp. Proc.* **1990**, *180*, 961.
- (18) Schmidt, H. K. *Inorganic and Organometallic Polymers*; ACS Symposium Series 360; American Chemical Society: Washington, DC, 1988; p 333.
- (19) Sanchez, C.; Ribot, F. *Comment. Inorg. Chem.* **1999**, *20*, 327.
- (20) Boilot, J. P.; Chaput, F.; Gacoin, T.; Malier, L.; Canva, M.; Brun, A.; Levy, Y.; Galaup, J. P. *C. R. Acad. Sci. Paris, Ser. IIB* **1996**, *322*, 27.
- (21) Judenstein, P.; Sanchez, C. *J. Mater. Chem.* **1996**, *6*, 54.
- (22) Schubert, U.; Hüsing, N.; Lorenz, A. *Chem. Mater.* **1995**, *7*, 2010.
- (23) Hüsing, N.; Schubert, U. *Angew. Chem., Int. Ed. Engl.* **1998**, *37*, 22.
- (24) Loy, D. A.; Shea, K. J. *Chem. Rev.* **1995**, *95*, 1431.
- (25) Baney, R. H.; Itoh, M.; Sakakibara, A.; Suzuki, T. *Chem. Rev.* **1995**, *95*, 1409.
- (26) Lindner, E.; Schneller, T.; Auer, F.; Mayer, H. A. *Angew. Chem., Int. Ed. Engl.* **1999**, *38*, 2154.
- (27) For a general survey, see: (a) *Hybrid Organic Inorganic Composites*; ACS Symposium Series 585; Mark, J. J. E., Lee, C. Y., Bianconi, P. A., Eds.; American Chemical Society: Washington, DC, 1995. (b) *New J. Chem.* (special issue) **1994**, *18*. (c) *Tailor-made Silicon Oxygen Compounds, From Molecules to Materials*; Corriu, R. J. P., Jützi, P., Eds.; Wieweg, Braunschweig, 1996.
- (28) Corriu, R. J. P.; Leclercq, D. *Angew. Chem., Int. Ed. Engl.* **1996**, *35*, 1420.
- (29) Corriu, R. J. P. *Polyhedron* **1998**, *17*, 925.
- (30) Corriu, R. J. P. *C. R. Acad. Sci. Paris, Ser. IIC* **1998**, 83.
- (31) Corriu, R. J. P.; Corriu, R. J. P. *Coord. Chem. Rev.* **1998**, *178–180*, 1051.
- (32) Corriu, R. J. P. *Angew. Chem., Int. Ed.* **2000**, *39*, 1376.
- (33) Anglaret, E.; Hasmy, A.; Jullien, R. *Phys. Rev. Lett.* **1995**, *75*, 4059.
- (34) Corriu, R. J. P.; Moreau, J. J. E.; Thépot, P.; Wong Chi Man, M.; Chorro, C.; Lère-Porte, J. P.; Sauvajol, J. L. *Chem. Mater.* **1994**, *6*, 640.
- (35) Corriu, R. J. P.; Moreau, J. J. E.; Thépot, P.; Wong Chi Man, M. *Chem. Mater.* **1992**, *4*, 1217.
- (36) Corriu, R. J. P.; Moreau, J. J. E.; Thépot, P.; Wong Chi Man, M. *J. Mater. Chem.* **1994**, *4*, 987.
- (37) Baugher, B. M.; Loy, D. A.; Prabakar, S.; Assink, R. A.; Shea, K. J.; Oviatt, H. *Mater. Res. Soc. Symp. Proc.* **1995**, *371*, 253.
- (38) Loy, D. A.; Baugher, B. M.; Prabakar, S.; Assink, R. A.; Shea, K. J. *Mater. Res. Soc. Symp. Proc.* **1995**, *371*, 229.
- (39) Bezombes, J. P.; Chuit, C.; Corriu, R. J. P.; Reyé, C. *J. Mater. Chem.* **1998**, *8*, 1749.
- (40) Bezombes, J. P.; Chuit, C.; Corriu, R. J. P.; Reyé, C. *J. Mater. Chem.* **1999**, *9*, 1727.
- (41) Dubois, G.; Corriu, R. J. P.; Reyé, C.; Brandès, S.; Denat, F.; Guillard, R. *Chem. Commun.* **1999**, 2283.
- (42) Shea, K. J.; Loy, D. A.; Webster, O. W. *Chem. Mater.* **1989**, *1*, 572.
- (43) Shea, K. J.; Loy, D. A.; Webster, O. W. *J. Am. Chem. Soc.* **1992**, *114*, 6700.
- (44) Small, J. H.; Shea, K. J.; Loy, D. A. *J. Non-Cryst. Solids* **1993**, *160*, 234.
- (45) Barrie, P. J.; Carr, S. W.; Li Ou, D.; Sullivan, A. C. *Chem. Mater.* **1995**, *7*, 265.
- (46) Carr, S. W.; Motevalli, M.; Li Ou, D.; Sullivan, A. C. *J. Mater. Chem.* **1997**, *7*, 865.
- (47) Cerveau, G.; Corriu, R. J. P.; Lepeyre, C. *J. Mater. Chem.* **1995**, *5*, 793.
- (48) Chevalier, P.; Corriu, R. J. P.; Moreau, J. J. E.; Wong Chi Man, M. *J. Sol-Gel Sci. Technol.* **1997**, *8*, 603.
- (49) Chevalier, P.; Corriu, R. J. P.; Delord, P.; Moreau, J. J. E.; Wong Chi Man, M. *New J. Chem.* **1998**, 423.
- (50) Boury, B.; Chevalier, P.; Corriu, R. J. P.; Delord, P.; Moreau, J. J. E.; Wong Chi Man, M. *Chem. Mater.* **1999**, *11*, 281.
- (51) Corriu, R. J. P.; Moreau, J. J. E.; Thépot, P.; Wong Chi Man, M. *Chem. Mater.* **1996**, *8*, 100.
- (52) Cerveau, G.; Corriu, R. J. P.; Dabiens, B. *J. Mater. Chem.* **2000**, *10*, 1113.
- (53) Oviatt, H. W., Jr.; Shea, K. J.; Small, J. H. *Chem. Mater.* **1993**, *5*, 943.
- (54) Chuit, C.; Corriu, R. J. P.; Dubois, G.; Reyé, C. *Chem. Commun.* **1999**, 723.
- (55) Dubois, G.; Reyé, C.; Corriu, R. J. P.; Chuit, C. *J. Mater. Chem.* **2000**, *10*, 1091.
- (56) Cerveau, G.; Corriu, R. J. P.; Lepeyre, C. *Chem. Mater.* **1997**, *9*, 2561.
- (57) Cerveau, G.; Corriu, R. J. P.; Costa, N. *J. Non-Cryst. Solids* **1993**, *163*, 226.
- (58) Audebert, P.; Cerveau, G.; Corriu, R. J. P.; Costa, N. *J. Electroanal. Chem.* **1996**, *413*, 89.
- (59) Corriu, R. J. P.; Hesemann, P.; Lanneau, G. *Chem. Commun.* **1996**, 1845.
- (60) Battioni, P.; Cardin, E.; Loulodi, M.; Schöllhorn, B.; Spyroulias, G. A.; Mansuy, D.; Traylor, T. G. *Chem. Commun.* **1996**, 2037.
- (61) Delmarre, D.; Bied-Charreton, C. *Sensors Actuators B* **2000**, *62*, 136.
- (62) Hobson, T. S.; Shea, K. J. *Chem. Mater.* **1997**, *9*, 616.
- (63) Corriu, R. J. P.; Moreau, J. J. E.; Wong Chi Man, M. *J. Sol-Gel Sci. Technol.* **1994**, *2*, 87.
- (64) Cerveau, G.; Corriu, R. J. P.; Lepeyre, C. *J. Organomet. Chem.* **1997**, *548*, 99.
- (65) Cerveau, G.; Corriu, R. J. P.; Dabosi, J.; Aubagnac, J. L.; Combarieu, R.; de Puyt, Y. *J. Mater. Chem.* **1998**, *8*, 1761.
- (66) Loy, D. A.; Baugher, B. M.; Baugher, C. R.; Schneider, D. A.; Rahimian, K. *Chem. Mater.* **2000**, *12*, 3624.
- (67) Lindner, E.; Kemmler, M.; Schneller, T.; Mayer, H. A. *Inorg. Chem.* **1995**, *34*, 5489.
- (68) Lindner, E.; Schneller, T.; Mayer, H. A.; Bertagnolli, H.; Ertel, T. S.; Hörner, W. *Chem. Mater.* **1997**, *9*, 1524.
- (69) Marsmann, H. *<sup>29</sup>Si NMR Spectroscopic Results*; Diehl, P., Fluck,

- E., Kosfeld, R., Eds.; Springer-Verlag: Berlin, 1981.
- (70) Williams, E. A. *NMR Spectroscopy of Organosilicon Compounds in the Chemistry of Organosilicon Compounds*; Patai, S., Rapoport, Z., Eds.; Wiley: New York, 1989; p 511.
- (71) Mägi, M.; Lippmaa, E.; Samoson, A.; Engelhardt, G.; Grimmer, A. R. *J. Phys. Chem.* **1984**, *88*, 1518.
- (72) Cerveau, G.; Corriu, R. J. P.; Lepeytre, C.; Mutin, P. H. *J. Mater. Chem.* **1998**, *8*, 2707.
- (73) Gregg, S. J.; Sing, S. W. *Adsorption, Surface Area and Porosity*; Academic Press: London, 1982.
- (74) Brunauer, S.; Emmet, P. H.; Teller, E. *J. Am. Chem. Soc.* **1938**, *60*, 309.
- (75) Brunauer, S.; Deming, L. S.; Deming, W. S.; Teller, E. *J. Am. Chem. Soc.* **1940**, *62*, 1723.
- (76) Barrett, E.; Joyner, L.; Halenda, P. *J. Am. Chem. Soc.* **1951**, *73*, 373.
- (77) Lepeytre, C. Ph.D. Dissertation, Montpellier, France, 1998.
- (78) Cerveau, G.; Corriu, R. J. P.; Fischmeister-Lepeytre, C. *J. Mater. Chem.* **1999**, *9*, 1149.
- (79) Cerveau, G.; Corriu, R. J. P.; Framery, E. *J. Mater. Chem.* **2000**, *10*, 1617.
- (80) Cerveau, G.; Corriu, R. J. P.; Framery, E. *Polyhedron* **2000**, *19*, 307.
- (81) Barton, T. J.; Bull, L. M.; Klemperer, W. G.; Loy, D. A.; McEnaney, B.; Misono, M.; Monson, P. A.; Pez, G.; Scherer, G. W.; Vartulli, J. C.; Yaghi, O. M. *Chem. Mater.* **1999**, *11*, 2633.
- (82) Cerveau, G.; Corriu, R. J. P.; Framery, E. *Chem. Commun.* **1999**, 2081.
- (83) Cerveau, G.; Corriu, R. J. P.; Framery, E. *J. Mater. Chem.* **2001**, *11*, 713.
- (84) Cerveau, G.; Corriu, R. J. P.; Framery, E. *C. R. Acad. Sci. Paris, Ser. Iic* **2001**, *4*, 79.
- (85) Boury, B.; Corriu, R. J. P.; Delord, P.; Le Strat, V. *J. Non-Cryst. Solids* **2000**, *265*, 41.
- (86) Boury, B.; Corriu, R. J. P.; Le Strat, V.; Delord, P.; Nobili, M. *Angew. Chem., Int. Ed.* **1999**, *38*, 3172.

CM011008Q